Nuclear Instruments and Methods in Physics Research B 272 (2012) 61–65

Contents lists available at ScienceDirect

Nuclear Instruments and Methods in Physics Research B

journal homepage: www.elsevier.com/locate/nimb

Structural and optical studies of Au doped titanium oxide films

E. Alves [a,b,*], N. Franco [a,b], N.P. Barradas [a,b], B. Nunes [a], J. Lopes [c], A. Cavaleiro [d], M. Torrell [e], L. Cunha [e], F. Vaz [e]

[a] Instituto Tecnológico e Nuclear (ITN), 2686-953 Sacavém, Portugal
[b] Centro de Física Nuclear da Universidade de Lisboa, Av. Gama Pinto, 21649-003 Lisboa, Portugal
[c] Instituto Superior de Engenharia de Lisboa, Portugal
[d] SEC-CEMUC – Universidade de Coimbra, Dept. Eng. Mecânica, Polo II, 3030-788 Coimbra, Portugal
[e] Centro de Física, Universidade do Minho, 4800-058 Guimarães, Portugal

ARTICLE INFO

Article history:
Available online 1 February 2011

Keywords:
Ion Implantation
TiO_2 films
Au nanoparticles
Rutherford backscattering spectrometry
Optical absorption

ABSTRACT

Thin films of TiO_2 were doped with Au by ion implantation and in situ during the deposition. The films were grown by reactive magnetron sputtering and deposited in silicon and glass substrates at a temperature around 150 °C. The undoped films were implanted with Au fluences in the range of 5×10^{15} Au/cm^2–1×10^{17} Au/cm^2 with a energy of 150 keV. At a fluence of 5×10^{16} Au/cm^2 the formation of Au nanoclusters in the films is observed during the implantation at room temperature. The clustering process starts to occur during the implantation where XRD estimates the presence of 3–5 nm precipitates. After annealing in a reducing atmosphere, the small precipitates coalesce into larger ones following an Ostwald ripening mechanism. In situ XRD studies reveal that Au atoms start to coalesce at 350 °C, reaching the precipitates dimensions larger than 40 nm at 600 °C. Annealing above 700 °C promotes drastic changes in the Au profile of in situ doped films with the formation of two Au rich regions at the interface and surface respectively. The optical properties reveal the presence of a broad band centered at 550 nm related to the plasmon resonance of gold particles visible in AFM maps.

1. Introduction

There has been a renewed interest in metal nanoparticles (NPs) embedded in dielectric matrices due to their potential applications in a wide range of high technological domains. These include areas as distinct as decorative objects (nanoparticles were used to provide different colours in roman glasses and medieval cathedrals windows for centuries) or nonlinear optics [1,2], bio and optical sensors [3,4], absorption components in solar cells and gas sensing systems [5]. Most of these applications are related with the optical resonances in the visible region of the electromagnetic spectrum due to the Surface Plasmon Resonance (SPR) absorption. The resonance frequency depends on size, morphology, shape and distribution, as well as on the particular dielectric characteristics of the surrounding medium in which the nanoparticles are dispersed [6,7]. As a result of the collective oscillations induced by the electromagnetic radiation on the conduction electrons at the surface of the nanoparticles the position and intensity of the SPR can be controlled by the volume fraction and size of the nanoparticles. The interaction between the particles can occur for high densities of the particles (volume fraction above ≈17%) [8] and a red shift of the SPR is observed with the size increase.

The production of the nanoparticles in the dielectric matrices can be achieved via in situ doping during the growth of the material or by ion implantation. While in situ doping is limited by thermodynamic solubility constraints ion implantation is free of any limitation offering several advantages to control the doping process. Several studies on ion implantation addressed the photocatalytic activity tailoring by implantation of N [9]. Also the doping with magnetic and other transition metals to extend the technological applications has been the subject of research during the last years [10,11]. However most of these studies were focused in single crystals and few reports deal with thin polycrystalline or amorphous films.

In this work we studied the structural and optical behaviour of TiO_2 thin films doped with Au nanoparticles. TiO_2:Au films were produced by reactive magnetron co-sputtering deposition process on silicon and glass substrates. Some undoped films were grown with the same conditions and subsequently implanted with Au ions for comparison. The precipitation of the Au nanoparticles was achieved with annealing in vacuum. The structural evolution of the TiO_2:Au system and the optical changes were studied after each annealing step with X-ray diffraction (XRD), atomic force microscopy (AFM), ion beam analysis (IBA) and optical absorption (OA).

* Corresponding author at: Instituto Tecnológico e Nuclear EN. 10, 2686-953 Sacavem, Portugal. Tel.: +351 219946086.
E-mail address: ealves@itn.pt (E. Alves).

0168-583X/$ - see front matter © 2011 Elsevier B.V. All rights reserved.
doi:10.1016/j.nimb.2011.01.033

2. Experimental details

The Au doped TiO_2 films were grown using two vertically opposed rectangular magnetrons disposed in a closed field configuration in the deposition chamber. The target was composed of a titanium (99.6% purity) with Au pellets (with a 40 mm^2 surface area and ~2 mm thickness), symmetrically incrusted in the erosion zone. The purity of the targets was confirmed by RBS results of the undoped films where no contaminations were found. A constant dc current density of 100 A m^{-2} was applied and an argon and oxygen mixture using 60 sccm (3×10^{-1} Pa) and 10 sccm (8×10^{-2} Pa) respectively, has been used. These conditions produce an approximately constant working pressure of 3.8×10^{-1} Pa during the deposition process. The deposition temperature was maintained nearly constant at 150 °C during the films growth. Substrate holder was placed in rotation at 6 rpm and in grounded conditions.

The undoped TiO_2 films, with a thickness of 75 nm, were grown with the same conditions (but without the Au pellets) and implanted with 150 keV Au ions to nominal fluences in the range 5×10^{15} cm^{-2}–1×10^{17} cm^{-2} at the high flux implanter of Instituto Tecnológico e Nuclear (ITN). The beam power density in the target was 0.1 W/cm^2 to minimize the heating effects. All the Au-doped films were annealed in vacuum (about 10^{-4} Pa) for 60 min in the temperature range of 200–800 °C. The samples cooled down to room temperature in vacuum.

The composition profiles of the as-deposited and annealed samples were measured by Rutherford backscattering spectroscopy (RBS) using a 2 MeV $^4He^+$ beam. The scattering angles were 140° (IBM geometry) and 180° at tilt angles 0° and 30°. The results were analysed with the IBA NDF code [12]. The crystalline structure of TiO_2 matrix and Au nanoclusters and the NPs size were investigated by X-ray diffraction (XRD), using a diffractometer (Cu-K_α radiation) operating in a Bragg–Brentano configuration. In situ XRD annealing studies were done using the hotbird difractometer at ITN with a step of 0.01° for 0.5 s. The optical properties (transmittance and absorvance) were characterized using a UV–Vis_NIR Spectrophotometer (Shimazu UV 2450 PC) in the spectral range from 250 nm to 1100 nm. Atomic force microscopy was used to characterize the shape, size and distribution of GNPs formed at the surface of the films during annealing at high temperature.

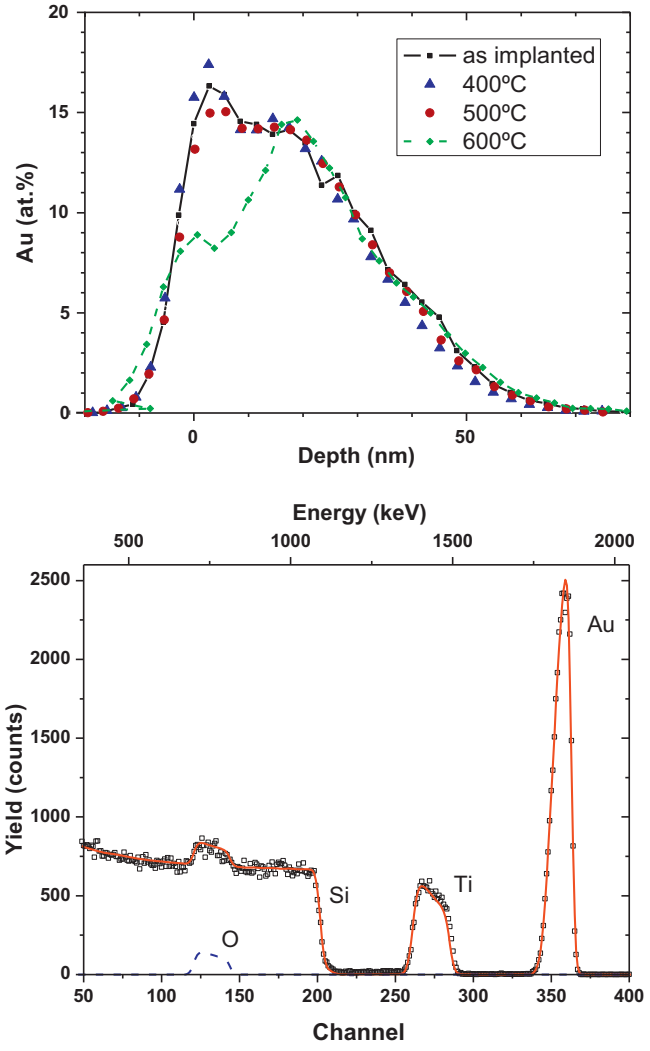

Fig. 1. Concentration profile of Au after implantation and annealing as indicated in the insert (top) and RBS spectrum measured after implantation and respective NDF simulation indicated by the continuous curve (bottom).

3. Results and discussion

3.1. Structural characterization

A typical RBS spectrum of a TiO_2 film implanted with a nominal fluence of 5×10^{16} cm^{-2} is shown in Fig. 1. The films are stoichiometric within 5% according to the NDF analysis of the RBS spectrum also included in the figure. In this particular case the Au profile has a maximum concentration of 15 at.% which is similar to the values obtained for the in situ doped samples (see Fig. 3). The film thickness is 75 nm and the Au is mostly concentrated in the first half. The Au profile is stable up to 500 °C with some surface loss observed during the annealing at 600 °C. For lower concentrations there was no evidence for changes in the implanted Au profile up to 800 °C. The thermal stability of Au implanted in dielectric matrices at 800 °C was also observed by other authors in sapphire (Al_2O_3) [13]. Also Shutthanandan et al. found similar results on Au implanted rutile single crystals annealed in air at 1000 °C [10].

For the sample implanted with 5×10^{16} cm^{-2} Au ions, XRD show a peak corresponding to the fcc Au(111) diffraction (ICDD card n° 04-0787), which proves that precipitation occurs during the implantation, Fig. 2. The peak position, integrated intensity and width were deconvoluted using Voigt functions to obtain information on the interplanar spacing and particle size. The results allow us to estimate a maximum dimension of 5 nm for the as implanted nanoparticles using the Scherrer formalism [14]. The formation of metallic nanoparticles in oxides during implantation was also observed in sapphire for fluencies above 5×10^{16} cm^{-2} [13].

In terms of the TiO_2 films, the XRD analysis fail to show any intense signal of diffraction suggesting the lack of long range order after the film deposition. However we cannot exclude the crystallization of the film by the fact that no relevant diffraction from the TiO_2 phases appear in Fig. 2 (some weak peaks were identified in the figure). Previous studies indicate that TiO_2 film crystallises into the anatase phase around 500 °C and a further increase of the temperature to 700 °C promotes the formation of the rutile phase and both phases can be present in the films [15]. In our case the reduced intensity of the TiO_2 peaks allied to the fact that the films are relatively thin can explain the difficulty to observe the diffraction peaks in the implanted samples.

The as grown films in situ doped show a nearly flat Au profile through the entire film thickness for concentrations up to 18 at.%. In some cases a higher concentration is found at the film-substrate interface which can be due to a relaxation of the solubility limits constraints caused by the mismatch of the two structures, Fig. 3. The Au profile remains unchanged during annealing at

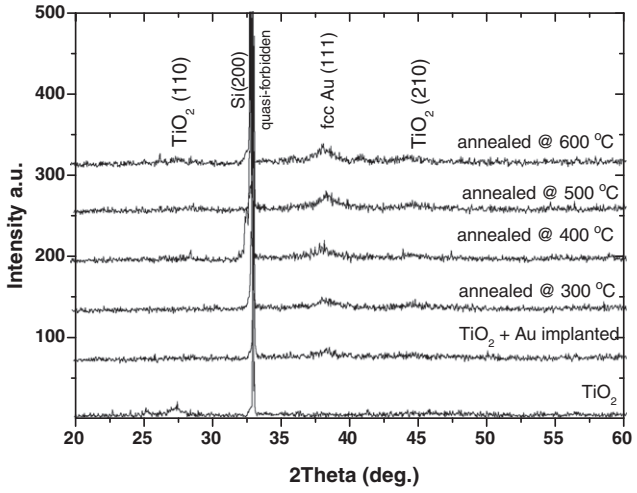

Fig. 2. Temperature dependence of XRD patterns of the TiO_2 film implanted with a fluence of 5×10^{16} $cm^{-2}Au^{+}$ ions. The peak showing the presence of Au nanoparticles is visible after implantation.

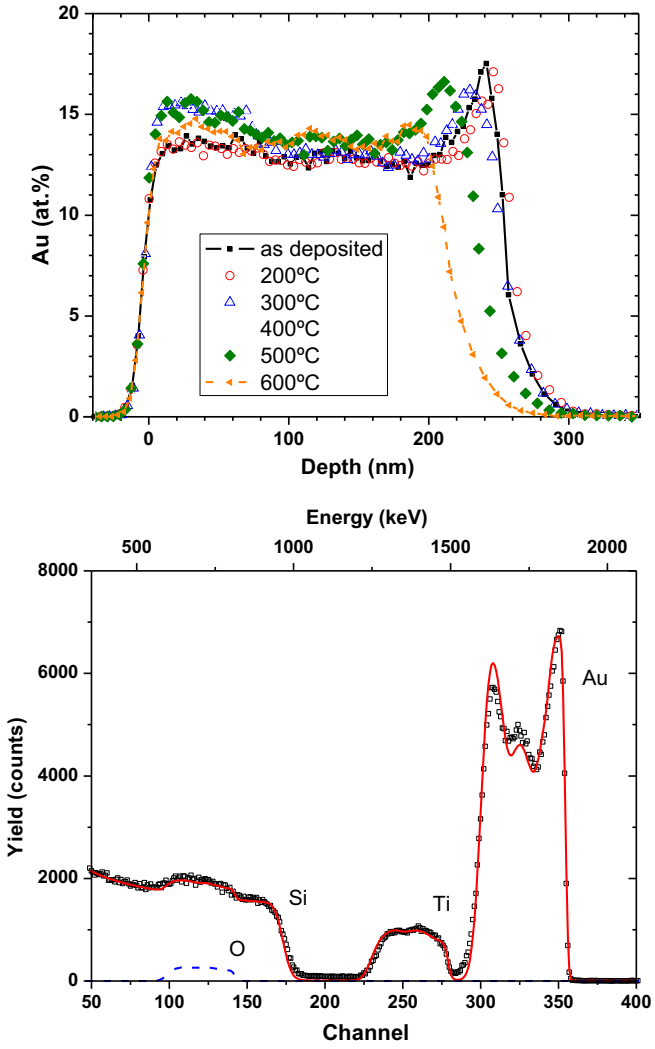

Fig. 3. Concentration profile of Au of in situ doped film after deposition and annealing as indicated in the insert (top) and RBS spectrum measured after annealing at 750 °C showing the Au diffusion (bottom). The continuous curve was obtained with the NDF code with a maximum concentration of 25 at.% of Au at the surface.

temperatures of 500 °C. At 600 °C we notice changes in the Au profile, revealing regions with different concentrations. This effect is very pronounced after annealing at 750 °C, which is illustrated in Fig 3(bottom). The changes observed in the Au profile are also related with the crystalline transformation of the TiO_2 film as discussed before. The in situ doped films do not show the formation of nanoparticles during the deposition process. At this stage the Au atoms are dissolved in the TiO_2 amorphous matrix structure. In situ XRD measurements indicate that the Au precipitation starts around 350 °C for the 15 at.% doped film, Fig. 4. The precipitation temperature varies with concentration and it was observed a decrease of the precipitation temperature with the increase of the Au concentration. From the peak width we estimate an initial particle size of 5–7 nm reaching 13–15 nm in the temperature range 400–500 °C. At the end of the annealing sequence Au particle size is greater than 30 nm but no accurate value could be determine using the Scherrer formalism. The results are in good agreement with the study of Vaz et al. [16] where they measured by TEM similar values for the Au nanoparticles within the same temperature ranges. The growth evolution was explained by the authors in terms of the Ostwald ripening coalescence mechanism. As we shown in Fig. 3b above 750 °C a fraction of Au diffuses towards the surface. To obtain information on the surface topography after the annealing, we did AFM scans in some samples. The results are indicated in Fig. 5 where the presence of large and perfectly spherical Au particles is observed. The formation of the Au spheres randomly distributed over the TiO_2 surface is an evidence of the low chemical affinity between the oxide and the Au atoms. A uniform size distribution of smaller particles (300 nm) buried in the TiO_2 surface are also visible in the figure. The height profile measured

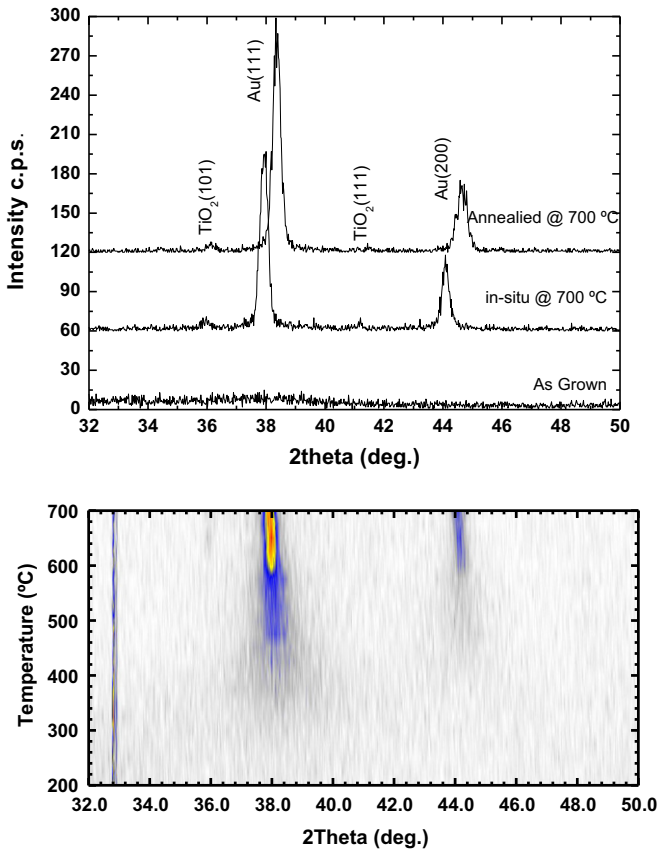

Fig. 4. In situ temperature dependence of XRD patterns of the TiO_2 film doped with 15 at.% Au. The peaks showing the presence of Au particles are visible after annealing at 350 °C.

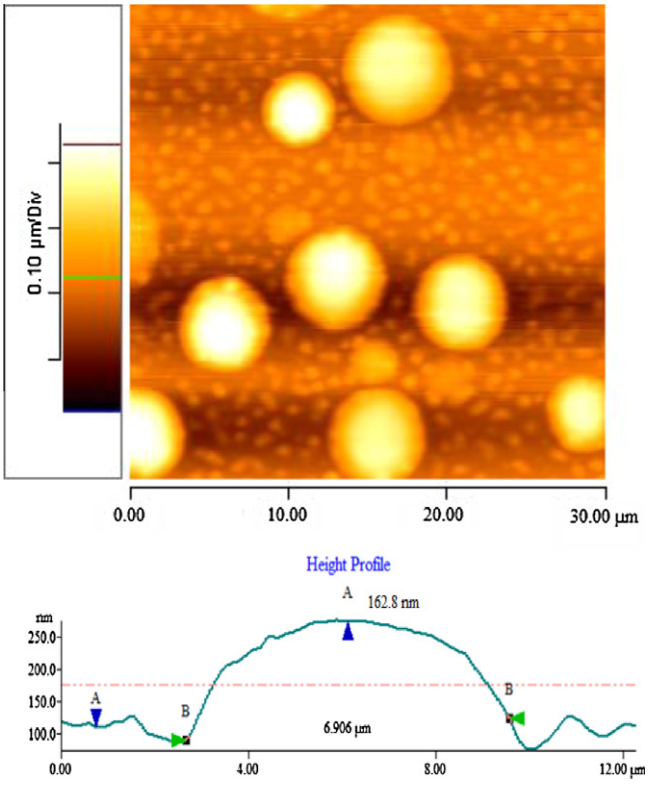

Fig. 5. AFM picture after annealing at 750 °C showing the Au particles at the surface. At bottom we show the topography of the top particle.

along one of the representative larger particles indicates an average radius of 6–7 µm while the smaller ones have 50 nm.

3.2. Optical characterization

The evolution of the reflectivity and absorption of the doped films was followed by spectrophotometry measurements. It is well known that the SPR is strongly influenced by the shape and size of the nanoparticles as well as by the coupling with the dielectric matrix. The as deposited films display a typical interference-like behaviour even for the in situ doped films. This confirms the structural analysis since no Au nanoparticles are expected to induce the SPR effect after the deposition. The implantation clearly affects the interference behaviour of the films which is attenuated and remains constant during the annealing treatments as shown in Fig. 6. The implantation also induces a colour change and for the highest fluences (above 5×10^{16} cm^{-2}) the interference disappears. This behaviour can be understood by the fact that at these fluences Au nanoparticles start to form in the film changing the medium and the interference conditions. Upon annealing above 200 °C the optical spectra of the implanted film with 5×10^{16} cm^{-2} start to reveal the presence of a broad band around 550 nm. This is the region where the SPR peak in the in situ TiO_2:Au-doped films was observed due to the presence of Au nanoparticles [15,16]. All these results suggest that for the implanted samples the annealing treatments are important to remove the defects produced by the implantation in order to enhance the SPR activity.

4. Conclusions

The study shows the viability to produce TiO_2 films doped with Au buried nanoparticles using ion implantation. This process offers the possibility to control the doping conditions presenting some

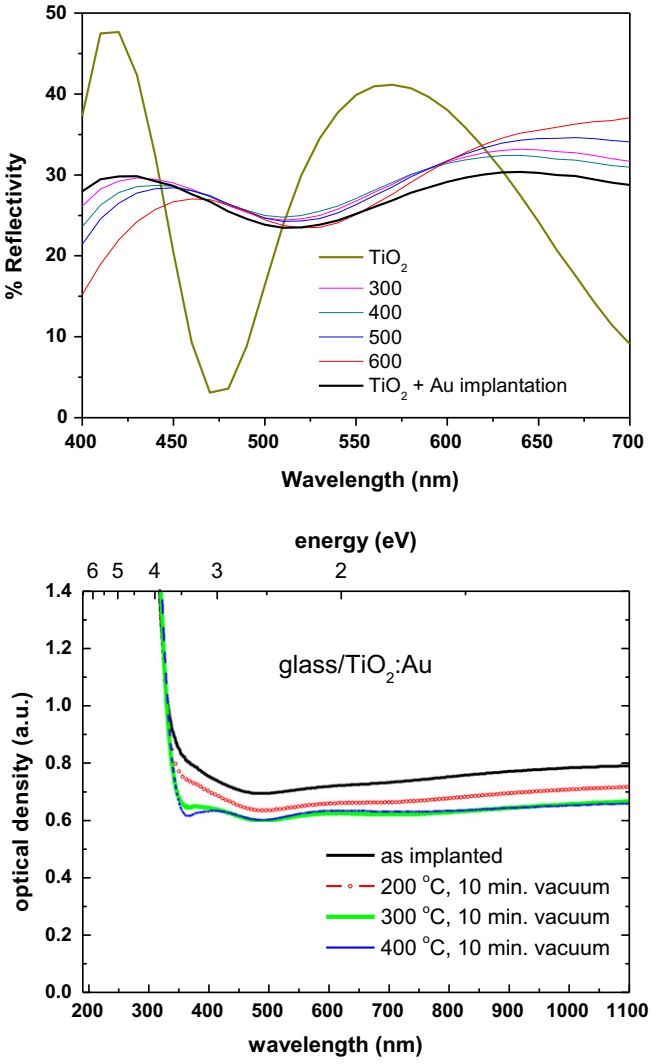

Fig. 6. Influence of the Au implantation and annealing temperature on the reflectivity (top) and absorption (bottom) for the sample implanted with the higher fluence.

advantages over the Au co-doping during the deposition. The results consistently show that the doped systems are stable up to temperatures of the order of 600 °C. The Au nanoparticles in the in situ doped films start to coalesce above 300 °C whereas for the implanted samples the precipitation occurs during the implantation at fluences above 5×10^{16} cm^{-2}. Above 700 °C Au starts to redistributed significantly inside the film leading to the formation of spherical particles at the surface with average diameters of 6–7 µm. The presence of the nanoparticles creates the conditions for the presence of a SPR band in the 550–600 nm region of the wavelength spectrum.

Acknowledgments

This research is sponsored by FEDER funds through the program COMPETE-Programa Operacional Factores de Competitividade and by national funds through Fundação para a Ciência e a Tecnologia, under the project PTDC/CTM/70037/2006.

References

[1] R.A. Ganeev, A.I. Ryasnyanskiĭ, A.L. Stepanov, T. Usmanov, C. Marques, R.C. Da Silva, E. Alves, Opt. Spectrosc. 101 (4) (2006) 615.

[2] G. Walters, I.P. Parkin, J. Mater. Chem. 19 (2009) 5–574.
[3] E. Hutter, J.H. Fendler, Adv. Mater. 16 (19) (2004) 1685.
[4] M. Torrell, P. Machado, L. Cunha, N.M. Figueiredo, J.C. Oliveira, C. Louro, F. Vaz, Surf. Coat. Technol. 204 (2010) 1569.
[5] R.M. Walton, D.J. Dwyer, J.W. Schwank, J.L. Gland, Appl. Surf. Sci. 125 (1998) 187.
[6] D. Dalacu, L. Martinu, J. Appl. Phys. 87 (1) (2000) 228.
[7] C.F. Bohren, D.R. Huffman, Absorption and Scattering of Light by Small Particles, Wiley Professional Paperback Edition, New York, 1998.
[8] T. Ung, L.M. Liz-Marzan, P. Mulvaney, J. Phys. Chem. B 105 (2001) 3441.
[9] Batzill Matthias, Erie Morales, Ulrike Diebold, Chem. Phys. 339 (36) (2007).
[10] V. Shutthanandan, Y. Zhang, C.M. Wang, J.S. Young, L. Saraf, S. Thevuthasan, Radiation effects and ion-beam processing of materials, in: MRS Proceedings, vol. 792, 2004, p. R11.5.1.
[11] J.V. Pinto, M.M. Cruz, R.C. da Silva, N. Franco, A. Casaca, E. Alves, M. Godinho, Eur. Phys. J. **B** 55 (2007) 253–260.
[12] N.P. Barradas, C. Jeynes, K.P. Homewood, B.J. Sealy, M. Milosavljevic, Nucl. Inst. Meth. B139 (1998) 235.
[13] C. Marques, E. Alves, R.C. da Silva, M.R. da Silva, A.L. Stepanov, Nucl. Inst. Meth. **B** 218 (139) (2004).
[14] C. Hammond, The Basics of Crystallography and Diffraction, International Union of Crystallography, Texts on Crystallography, vol. 3, Oxford University Press, New York, 1997.
[15] M. Torrell, L. Cunha, A. Cavaleiro, E. Alves, N.P. Barradas, F. Vaz, Appl. Surf. Sci. 256 (2010) 6536.
[16] M. Torrell, L. Cunha, M.R. Kabir, A. Cavaleiro, M.I. Vasilevskiy, F. Vaz, Mat. Lett. 64 (2624) (2010).